

The Elastic Modulus of Steel Fiber Reinforced Concrete (SFRC) with Random Distribution of Aggregate and Fiber

Shadafza, E.¹ and Saleh Jalali, R.^{2*}

¹ M.Sc. Student, Department of Civil Engineering, Faculty of Engineering, University of Guilan, Rasht, Iran.

² Assistant Professor, Department of Civil Engineering, Faculty of Engineering, University of Guilan, Rasht, Iran.

Received: 21 Aug. 2014;

Revised: 28 Dec. 2015;

Accepted: 30 Dec. 2015

ABSTRACT: The present paper offers a meso-scale numerical model to investigate the effects of random distribution of aggregate particles and steel fibers on the elastic modulus of Steel Fiber Reinforced Concrete (SFRC). Meso-scale model distinctively models coarse aggregate, cementitious mortar, and Interfacial Transition Zone (ITZ) between aggregate, mortar, and steel fibers with their respective material properties. The interfaces between fibers and mortar have been assumed perfectly bonded. Random sampling principle of Monte Carlo's simulation method has been used to generate the random size, orientation, and position of aggregate particles as well as steel fibers in concrete matrix. A total of 2100 two-dimensional and three-dimensional cube specimens (150 mm) with varying volume fractions of aggregate and fiber have been randomly generated. The commercial code ABAQUS has been used to analyze the specimens under tensile loading and the calculated elastic modulus has been compared to other analytical and experimental values. Results indicate that the non-homogeneity of the matrix and random distribution of aggregate and fibers manage to disperse calculated efficiency factor of fiber with a standard deviation of 2.5% to 3.0% (for 150 mm cube specimens, it can be different for other specimens). Nevertheless, the mean value of the calculated efficiency factor agrees well with the value, recommended by Hull (1981), for uniformly-distributed fibers, equal to 0.353, and 0.151 for two and three-dimensional models respectively.

Keywords: Aggregate, Elastic Modulus, Mesoscopic, Random Distribution, Steel Fiber Reinforced Concrete.

INTRODUCTION

Fiber Reinforced Concrete (FRC) is currently used in a wide range of applications, such as bridge decks, airport pavements, tunnels, etc. FRC is a kind of concrete, primarily made from hydraulic

cements, aggregate particles, and discrete reinforcing fibers, with various tests taken to determine the actual characteristics and advantages of fibrous materials. Fibers, suited for the reinforcing composites, have been made from steel, glass, and organic polymers. Steel Fiber Reinforced Concrete

* Corresponding author E-mail: saleh@guilan.ac.ir

(SFRC) has advantages over traditionally-reinforced one in civil engineering. Reinforcement by steel fibers can improve the reinforced concrete structures' resistance to shrinkage cracking along with their durability (Bernardi et al., 2013; Salehian et al., 2014; Islam et al., 2014; Ding, 2011; Wang et al., 2011; Tailhan et al., 2015; Yazici et al., 2013; Rashid-Dadash, 2014). According to Zaitsev and Wittmann, (1981) there are several hierarchical levels of multi-phase microstructural analysis, namely macro-level, meso-level, micro-level, and nano-level. At macro-level, the concrete is regarded as a homogeneous material with smeared cracks while at meso-level it is treated as consisting of a coarse aggregate, mortar matrix with fine aggregate dissolved in it, and interfacial zones between the aggregate and the mortar matrix (Ulm and Jennings, 2008; Hung et al., 2008; Smilauer and Krejci, 2009; Smilauer and Bazant, 2010; Gal and Kryvoruk, 2011; Comby-Peyrot et al., 2009; Grassl et al., 2012; Grassl and Jirasek, 2010; Grassl and Rempling, 2008; Huang et al., 2015; Nguyen et al., 2015; Qin and Zhang, 2011; Roubin et al., 2015; Skarzynski and Tejchman, 2010; Shahabeyk et al., 2011; Sun et al., 2015; Titscher and Unger, 2015; Xu et al., 2012a; Wang et al., 2015; Wu et al., 2015; Zhou and Hao, 2009).

At micro-level, the mortar matrix of the previous level is subdivided into fine aggregate and hardened cement pastes with pores, embedded inside whereas at nano-level, the hardened cement paste is further divided into big pores (air voids) and hardened cement paste with only small pores (capillary pores) in it. Thanks to current computerized capabilities and computational mechanic technology, some researchers have performed numerical simulations of static and dynamic responses of the cementitious material (Özcan et al., 2009; Teng et al., 2007; Wang et al., 2009). Meso-scale

models with distinctive considerations of aggregate and mortar have been developed by other researchers to simulate concrete tests by both static (Wriggers and Mofteh, 2006; Kim and Abu, 2010; Rizzuti, 2014) and dynamic loading (Zhou and Hao, 2008a; Zhou and Hao, 2008b; Hao et al., 2009; Zhang, 2013). It was found that meso-scale model provides a more realistic representation of concrete material properties, yielding more reliable simulations of concrete failure mechanisms and material properties than the homogenous model. Xu et al. (2012b) have developed a meso-scale numerical model to investigate the effects of aggregate distribution, fiber distribution, and fiber dosage on the overall compressive strength and crack initiation and propagation in FRC under impact loading. Also numerous theories have been developed to predict the behavior of composite materials, starting with the various effective properties, obtained by the models of Mori and Tanaka (1973), and including self-consistent approaches of Hill (1965) as well as various mathematical homogenization methods (Gal and Kryvoruk, 2011) with Ahmad and Lagoudas (1991) and Teng et al. (2004) suggesting empirical formulation to evaluate the elastic properties of FRC.

The present paper offers a meso-scale numerical model to investigate the effects of aggregate and fiber random distribution on the elastic modulus of SFRC. In the meso-scale model, coarse aggregate, cementitious mortar, Interfacial Transition Zone (henceforth ITZ) between aggregate and mortar, and steel fibers are distinctively modeled with their respective material properties. The coarse aggregate particles are assumed to have angular and spherical shapes in 2D and 3D specimens respectively with randomly-distributed sizes, orientations, and locations. AutoCAD and VBA have been utilized to generate the

random sizes, orientations, and positions of aggregate particles and steel fibers in concrete matrix with the interfaces between fibers and mortar, assumed to be perfectly bonded. The commercial code ABAQUS has been employed to analyze the specimens under tensile loading. The calculated elastic modulus is compared with other analytical and experimental values to verify the accuracy.

Random Generation of Aggregate Particles and Fibers

In this study, meso-scale models of 2D, and 3D specimens with angular and spherical aggregate particles, respectively, and steel fibers are developed to simulate the specimens with different dosages of aggregate particles and fibers. In 2D specimens, for a given type of angular aggregate, the shape of which has been prescribed (Figure 1), the major factors to be considered in the generation of random aggregate structure are the rotation, size, and spatial distribution of the particles. Meanwhile in 3D specimens with spherical aggregate particles, random sizes and positions of the particles should be taken into consideration. For so doing, the random sampling principle of Monte Carlo's simulation method has been used, which is done by taking samples of aggregate particles from a source, whose size distribution follows Fuller's grading curve (Figure 2) and placing the aggregate particles into the concrete one by one in such a way that they will not overlap with the particles, already placed, and the spatial distribution is as macroscopically homogeneous as possible. This method is commonly called the take-and-place method (Wang et al., 1999). The take-process and place-process are performed concurrently in the sense that a particle generated by the take-process is immediately placed into the concrete. They are conducted in a sequence,

starting with the largest size particles until the last particle of the size range, then to be repeated for successively-smaller size particles, as it is generally easier to pack the particles into the concrete in this way. After random distribution of aggregate particles, fibers are distributed randomly between aggregate particles and within mortar in such a way that they, too, will not overlap with the aggregate particles, already placed. The 2D and 3D specimen size is $150 \times 150 \text{ mm}^2$, and $150 \times 150 \times 150 \text{ mm}^3$, with the minimum and maximum size of coarse aggregate, assumed to be 8 and 20 mm; and the length and diameter of steel fibers, taken to be 30 and 1.0 mm respectively. The taking and placing process of aggregate particles and fibers to generate random specimens is summarized as follows:

Step 1. Calculate the volume of aggregate to be generated in a certain grading segment.

Step 2. Randomly generate the position, rotation, and diameter of aggregate particle within the corresponding segment.

Step 3. Check to ensure that the generated aggregate is within the specimen boundary and does not overlap with other aggregate particles that have been already placed in the specimen. Otherwise, discard this aggregate and perform a new generation until it satisfies the above conditions.

Step 4. Repeat Steps 2 and 3 until the volume of generated aggregate particles is equal to the calculated volume of aggregate for the specified grading segment.

Step 5. Repeat Steps 1 to 4 for all grading segments.

Step 6. Calculate the quantity of fibers, in accordance with the volume of fiber dosage.

Step 7. Generate the random fiber position and orientation, and place the fiber in the specimen.

Step 8. Check to ensure the fiber is located within the specimen boundary and does not overlap with aggregate particles that have been already placed in the

specimen. Otherwise, discard this fiber and perform a new generation until it satisfies the above conditions.

Step 9. Repeat Steps 8 and 9 until the volume of the total fibers is equal to the specified fiber volume.

Figures 3 and 4 indicate a sample of generated models of 2D and 3D specimens.



Fig. 1. Different shapes of aggregate for 2D models

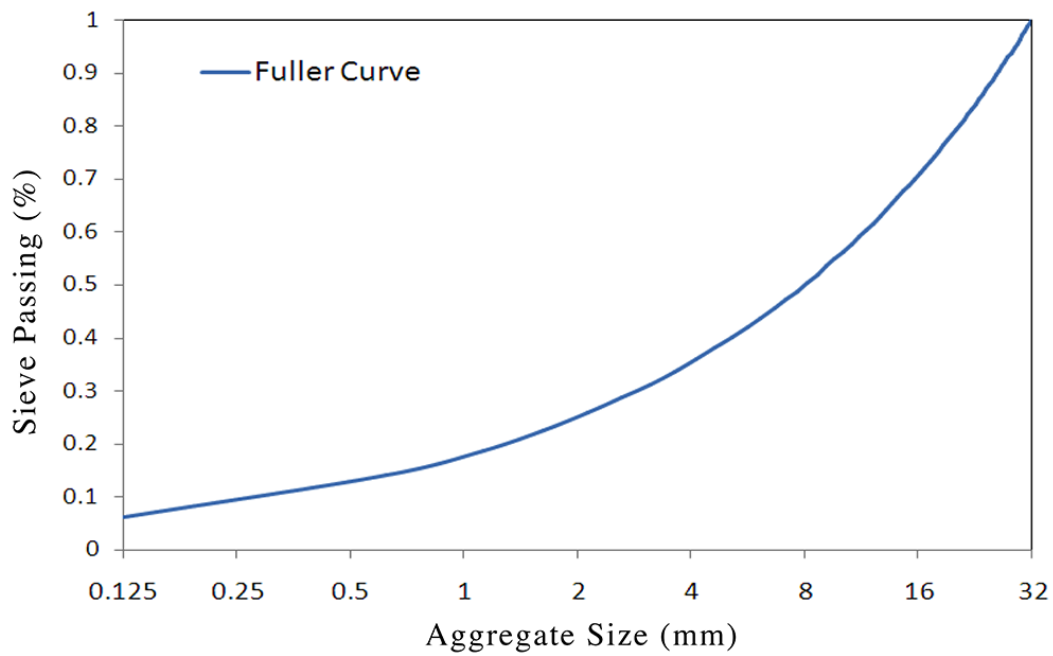


Fig. 2. Fuller grading curve

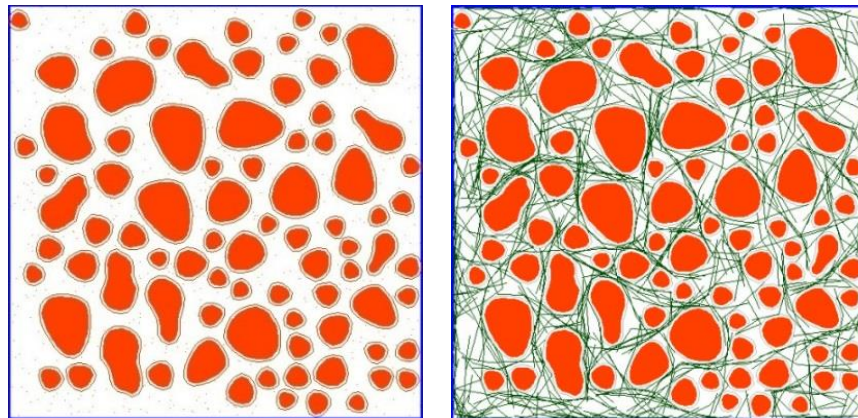


Fig. 3. A sample of generated model of 2D specimen, $150 \times 150 \text{ mm}^2$ in size

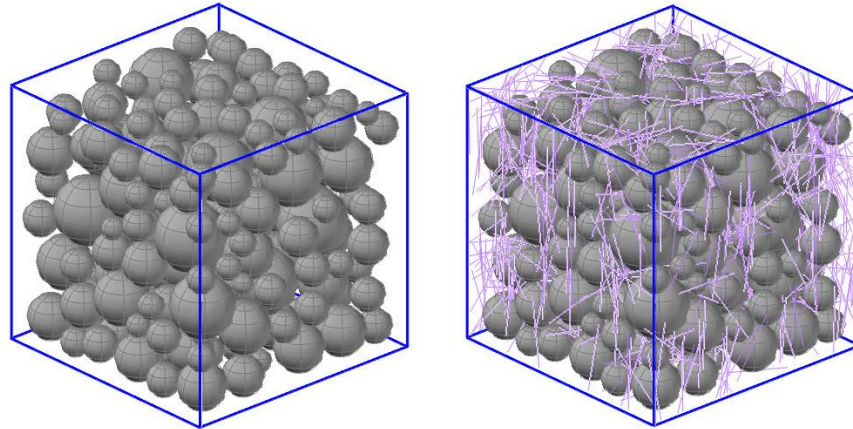


Fig. 4. A sample of generated model of 3D specimen, $150 \times 150 \times 150 \text{ mm}^3$ in size

Finite Element Model

In order to carry out a linear analysis of the randomly-generated specimens under direct tension, 2D and 3D models of SFRC specimens are constructed and modeled in ABAQUS. Modulus of elasticity and Poisson's ratio for elastic material property of aggregate, mortar, ITZ, and steel fiber are considered within the range of other studies' assumptions, presented in Table.1 (Jing, 2011; Gal, 2011). Many researches have been done to study the properties of ITZ but this field is yet to be known thoroughly. The thickness of the ITZ is about 0.05 mm (Zheng, 2005) but due to computer-processing time difficulties, it is considered to be 1 mm. It is assumed that within the ITZ

area, the material properties are weaker than the mortar matrix; however, in order to compensate the increased thickness of ITZ, the ITZ material is not considered quite weaker than the mortar and is regarded as a homogenized combination of mortar and ITZ. ABAQUS' auto-meshing with a maximum size of 3 mm has been employed to mesh the specimens that become finer near the aggregate particles. Elements, used for modeling aggregate, mortar, and ITZ, are 3-Node linear plane stress triangles (CPS3) as well as 4-Node linear tetrahedrons (C3D4) for 2D and 3D specimens, respectively. Fibers are modeled by 2-Node linear 2-D truss elements (2DT2) which are embedded in mortar (Figures 5 and 6).

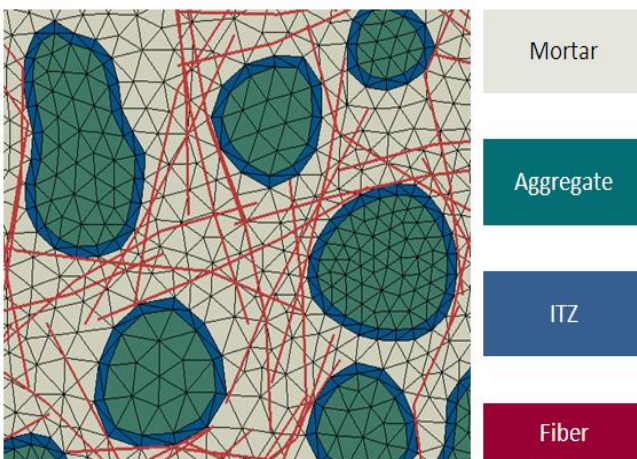


Fig. 5. 2D Finite Element model of SFRC specimen

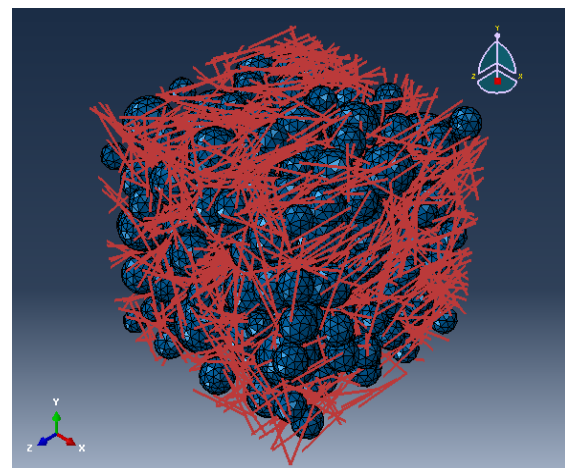


Fig. 6. 3D Finite Element model of SFRC specimen

Table 1. Material properties of SFRC specimens

	Mortar	Aggregate	ITZ	Fiber
Modulus of Elasticity (GPa)	19	70	15	200
Poisson's Ratio	0.2	0.2	0.2	0.3

RESULTS AND DISCUSSION

To estimate the tensile modulus of a short-fiber composite, Cox (1952) proposed a theory that assumes a completely elastic transfer of stresses from the matrix to the fiber. It considers an ideal case of short fibers, aligned with the stress direction, and is arranged in a particular pattern (e.g., a square or a hexagonal array). The theory derives the distribution of tensile stress within the fiber, along its axial direction. By averaging the stress distribution within the fibers, it predicts the tensile modulus for aligned short-fiber composites, in the direction of alignment, which is equal to:

$$E_{cf} = V_m E_m + \chi_2 V_f E_f \quad (1)$$

where

$$\chi_2 = 1 - \frac{\tanh(n_c s)}{n_c s}, n_c = \sqrt{\frac{2G_m}{E_f \ln(2R/d)}} \quad (2)$$

$$G_m = \frac{E_m}{2(1+\nu_m)}, \frac{2R}{d} = \sqrt{\frac{\pi}{4V_f}}, s = \frac{l}{d}$$

where χ_2 : is fiber-length correction factor, s : is the aspect ratio for fibers of length, l and diameter d , R : is the fiber-packing distance, G_m : is the matrix shear modulus, ν_m : is the matrix Poisson ratio, E_f and E_m : are the fiber and matrix tensile modulus, and V_f and V_m : are the fiber and matrix volume fractions, respectively. When fibers are not perfectly aligned with the stress direction, an orientation-efficiency factor χ_1 is added to Eq. (1) (Hull, 1981).

$$E_{cf} = V_m E_m + \chi_1 \chi_2 V_f E_f, 0 < \chi_1 < 1 \quad (3)$$

For two and three-dimensional uniformly-distributed fiber orientations, the orientation efficiency factor is $\chi_I = 0.375$ and $\chi_I = 0.2$.

In this paper the matrix is non-homogenous and contains mortar, coarse aggregate, and ITZ. The effects of random distribution of aggregate particles and fibers on the tensile modulus of SFRC are investigated. For this purpose 300 two and three-dimensional specimens with different volume fractions of aggregate and fibers (2100 specimens in total) are randomly generated. The volume fraction of aggregate and fibers varies from 30 to 50% and 0 to 4% respectively (Wriggers and Moftah, 2006; Wang et al., 2009; Rizzuti, 2014).

Figures 7 and 8 show the variations of calculated tensile modulus of SFRC with respect to the volume fractions of aggregate and fiber. As it is expected, by increasing the volume fractions of aggregate and fibers, the modulus of elasticity of SFRC rises. As it is seen the effect of fiber on modulus of elasticity for two-dimensional models is more than that of the three-dimensional ones.

In Figures 9 and 10 the influence of steel fibers on tensile modulus of all generated specimens are shown and compared with other analytical values and experimental data. In these figures, the vertical axis is multiplied by the value of fiber efficiency factor to fiber volume ($\chi V_f = \frac{E_{cf} - V_m E_m}{E_f}$) and the horizontal axis is the fiber volume fraction (V_f), thus each line's slope indicates the efficiency factor of the fiber ($\chi = \chi_1 \chi_2$). As it can be seen, the

calculated values of the fiber efficiency factor show some dispersion with a mean value of μ and a standard deviation of $\sigma(\chi = \mu \pm \sigma)$. Also, other researcher's recommendations of fiber efficiency factor have been shown with lines (the slope of each line is the fiber efficiency factor value). The fiber efficiency factors, suggested by

Teng et al. (2004) and Gal (2011) are equal to 0.34 and 0.33, respectively, being very close to the ones, proposed by Williamson (1974) ($\chi = 0.35$). Therefore these results have been obviously eliminated from the figure and the results of Williamson (1974) represent those of Teng et al. (2004) and Gal (2011).

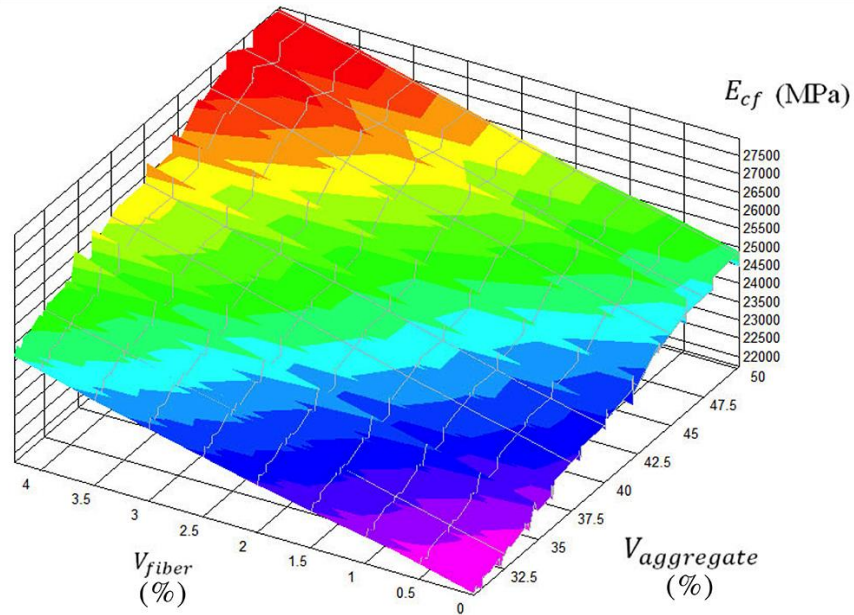


Fig. 7. Tensile modulus of 2D specimens of SFRC with different volume fractions of aggregate and fibers

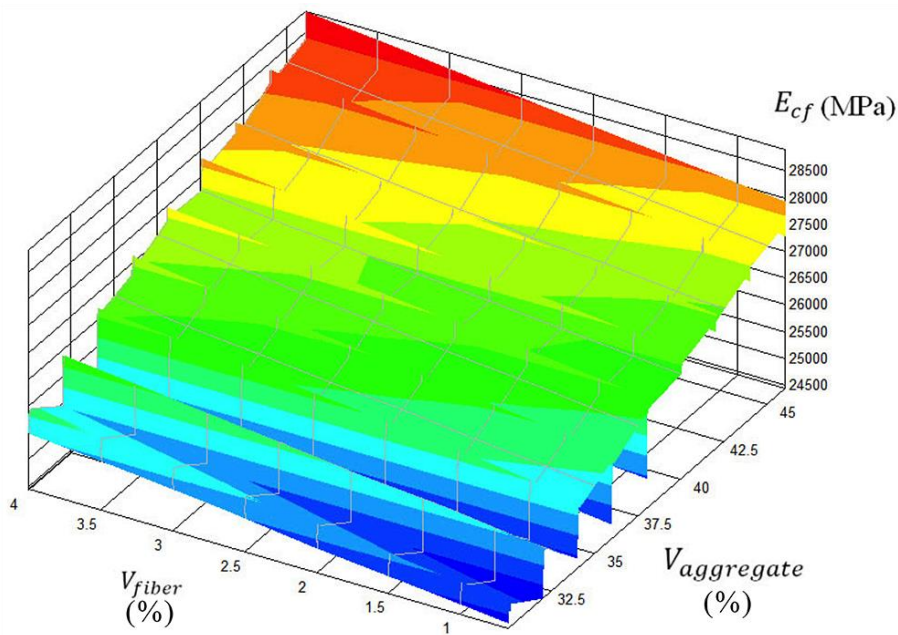


Fig. 8. Tensile modulus of 3D specimens of SFRC with different volume fractions of aggregate and fibers

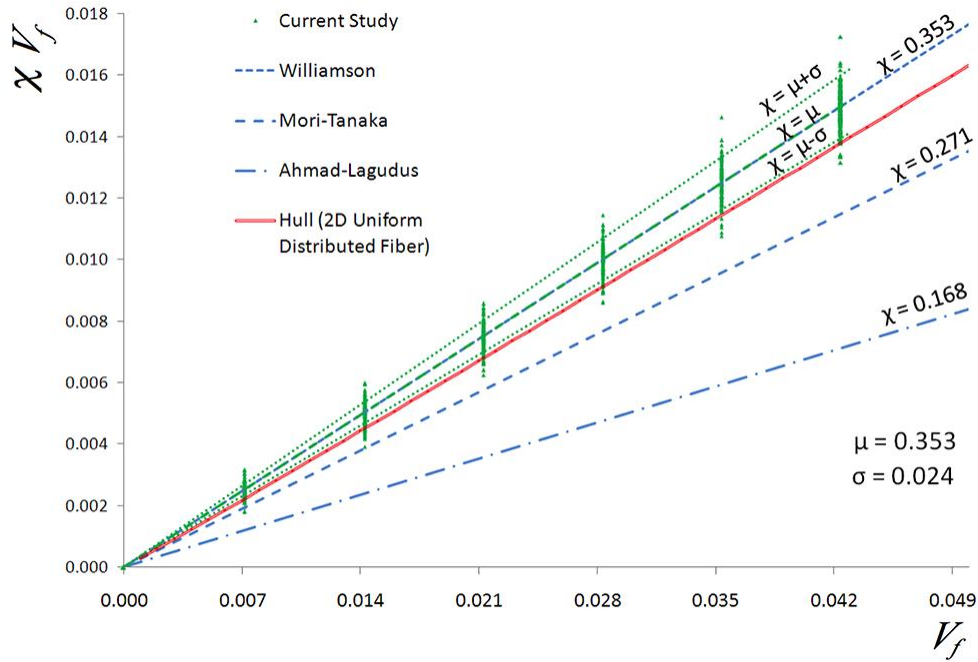


Fig. 9. Influence of steel fiber volume fraction on elastic modulus of 2D models

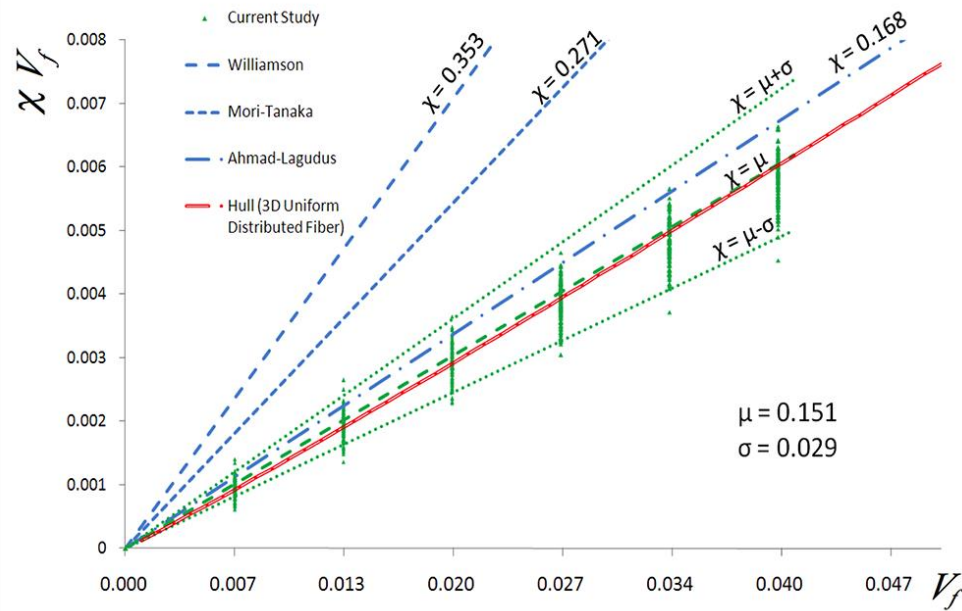


Fig. 10. Influence of steel fiber volume fraction on elastic modulus of 3D models

In Figure 9 for 2D models the mean value of the calculated efficiency factor of fiber is $\mu = 0.353$ with a standard deviation of $\sigma = 0.024$, which agrees with the experimental results of Williamson (1974) but surpasses those of Mori-Tanaka (1973),

and Ahmad and Lagoudas (1991). The mean value is slightly larger than the value, recommended by Hull (1981) for 2D uniformly-distributed fibers ($\chi = 0.323$). In Figure 10 for 3D models the mean value of the calculated efficiency factor of fiber is

$\mu = 0.151$ with a standard deviation of $\sigma = 0.029$, which agrees with the recommended values of Ahmad and Lagoudas (1991) but is smaller than the experimental values of Williamson (1974) as well as those, recommended by Mori-Tanaka (1973). What is more, the mean value is in good agreement with the recommended values of Hull (1981) for 3D uniformly-distributed fibers ($\chi = 0.149$).

In Figures 11 and 12 compare the calculated efficiency factor of fiber by finite element analysis to the one, determined by Eq. (3) and suggested by Hull (1981), for 2D and 3D models, respectively. As it can be seen in Figure 11, most of the points are scattered above the bisector line, which means that most of the calculated efficiency factors by finite element analysis are larger than those, suggested by Hull (1981) for 2D models. In Figure 12, however, they are

below the bisector line, meaning that most of calculated efficiency factors are smaller than the suggested factors of Hull for 3D models. This difference can be discussed, based on the fact that based on the theory of Cox (1952) and Hull (1981), the matrix was supposed to be homogenous with only the random orientation of fibers, taken into considered. On the contrary, the matrix in this study is non-homogenous, containing mortar, coarse aggregate, and ITZ. So the random orientation and position of aggregate particles and fibers influence each other simultaneously which scatters the calculated factors with a standard deviation of 2.5% to 3.0% (for 150 mm cube specimens, while it can vary with other specimens). Nevertheless the mean value of the calculated efficiency factor is in good agreement with the value, recommended by Hull (1981) for uniformly-distributed fibers.

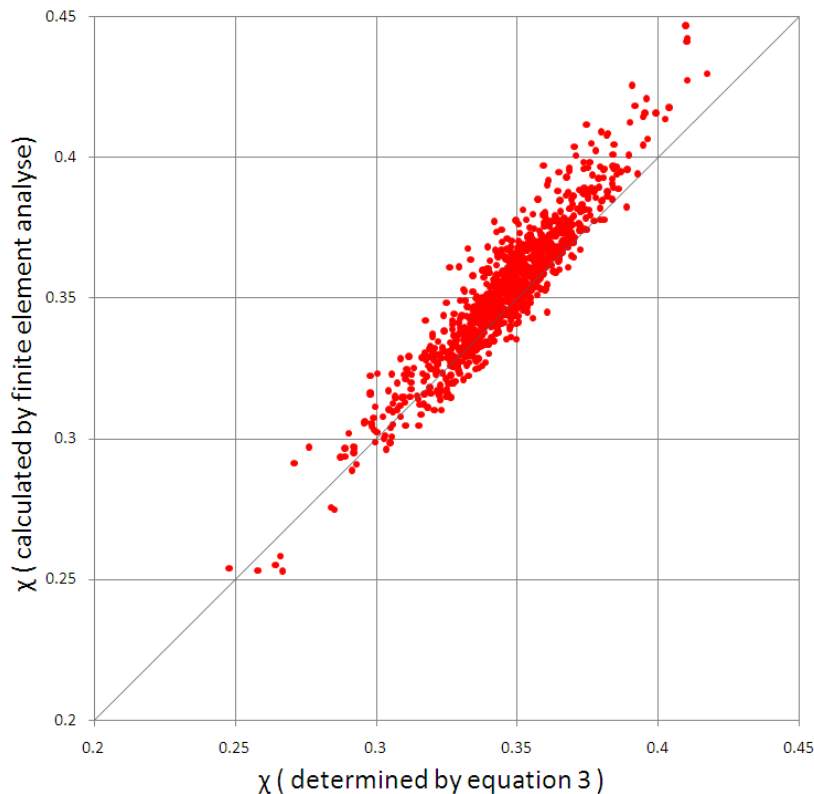


Fig. 11. Comparison between calculated efficiency factors and those, determined by Eq. (3) and suggested by Hull for 2D models

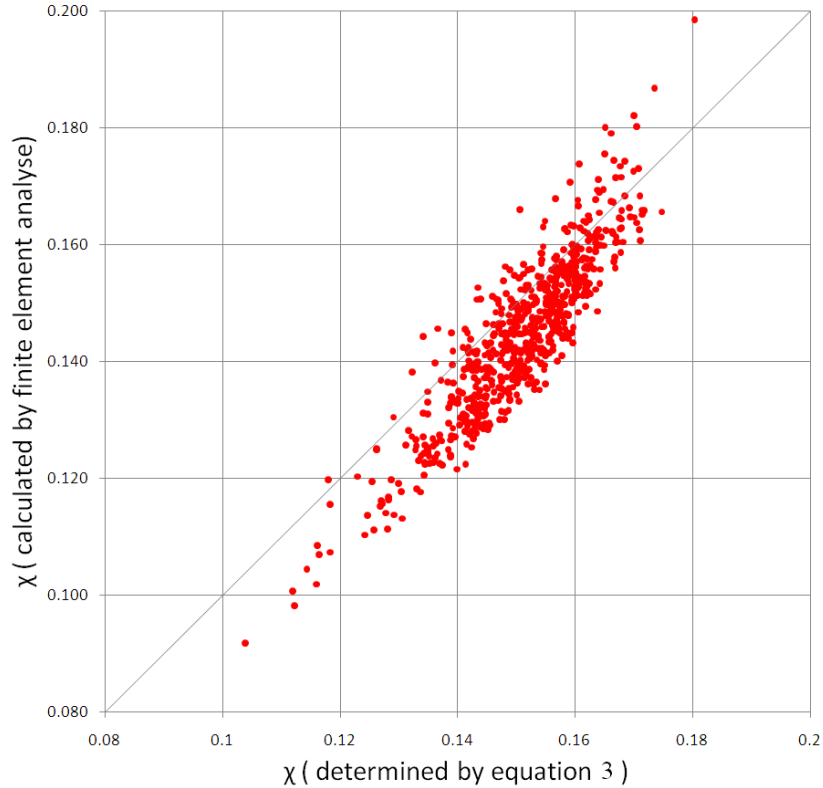


Fig. 12. Comparison between calculated efficiency factors and those, determined by Eq. (3) and suggested by Hull for 3D models

CONCLUSIONS

A sum of 2100 two and three-dimensional specimens with different volume fractions of aggregate and fiber have been generated by random sampling principle of Monte Carlo's simulation method, in which the commercial code, ABAQUS, has been used to analyze the specimens under tensile loading. Results show that the non-homogeneity of the matrix and random distribution of aggregate particles and fibers lead to a dispersion of calculated efficiency factors of fiber with a standard deviation of 2.5% to 3.0%. Nevertheless the mean value of the calculated efficiency factor agrees with the recommended value of Hull (1981) for uniformly distributed fibers, and is equal to 0.353 and 0.151 for two and three-dimensional models respectively.

REFERENCES

- Ahmad, H.A. and Lagoudas, C.L. (1991). "Effective elastic properties of fiber-reinforced concrete with random fibers", *Journal of Engineering Mechanics*, 117(12), 2931-2938.
- Bernardi, P., Cerioni, R. and Michelini, E. (2013). "Analysis of post-cracking stage in SFRC elements through a non-linear numerical approach", *Engineering Fracture Mechanics*, 108, 238-250.
- Comby-Peyrot, I., Bernard, F., Bouchard, P., Bay, F. and Garcia-Diaz, E. (2009). "Development and validation of a 3D computational tool to describe concrete behavior at meso-scale; application to the alkali-silica reaction", *Computational Material Science*, 46, 1163-1177.
- Cox, H.L. (1952). "The elasticity and strength of paper and other fibrous materials", *British Journal of Applied Physics*, 3(3), 72-79.
- Ding, Y. (2011). "Investigations into the relationship between deflection and crack mouth opening displacement of SFRC beam", *Construction and Building Materials*, 25(5), 2432-2440.

- Gal, E. and Kryvoruk, R. (2011). "Fiber reinforced concrete properties; a multiscale approach", *Computers and Structures*, 8(5), 525-539.
- Grassl, P., Gregoire, D., Solano, L.R. and Pijaudier-Cobat, G. (2012). "Meso-scale modeling of the size effect on fracture process zone of concrete", *International Journal of Solids and Structures*, 49(13), 1818-1827.
- Grassl, P. and Jirasek, M. (2010). "Meso-scale approach to modeling the fracture process zone of concrete subjected to uniaxial tension", *International Journal of Solids and Structures*, 47(13), 957-968.
- Grassl, P. and Rempling, R. (2008). "A damage-plasticity interface approach to the meso-scale modeling of concrete subjected to cyclic compressive loading", *Engineering Fracture Mechanics*, 75(16), 4804-4818.
- Hao, Y.F., Hao, H. and Li, Z.X. (2009). "Numerical analysis of lateral inertial confinement effects on impact test of concrete compressive material properties", *International Journal of Protective Structures*, 1(1), 143-145.
- Hill, R. (1965). "A self-consistent mechanics of composite materials", *Journal of Mechanics and Physics of Solids*, 13(4), 213-222.
- Huang, Y., Yang, Z., Ren, W., Liu, G. and Zhang, C. (2015). "3D meso-scale fracture modeling and validation of concrete based on in-situ X-ray Computed Tomography images using damage plasticity model", *International Journal of Solids and Structures*, 67-68, 340-352.
- Hull, D. (1981). *An introduction to composite materials*, Cambridge University Press, London.
- Hung, L.T., Dormieux, L., Jeannin, L., Burlion, N. and Barthélémy, J.F. (2008). "Nonlinear behavior of matrix-inclusion composites under high confining pressure: application to concrete and mortar", *Comptes Rendus Mécanique*, 336(8), 670-676.
- Islam, M., Khatun, S., Islam, R., Dola, J.F., Hussan, M. and Siddique, A. (2014). "Finite Element analysis of Steel Fiber Reinforced Concrete (SFRC): Validation of experimental shear capacities of beams", *Procedia Engineering*, 90, 89-95.
- Jing, Li., Lin-fu, W., Lin, J., Juan, L. and Hu, L. (2011). "Numerical simulation of uniaxial compression performance of big recycled aggregate-filled concrete", *Electric Technology and Civil Engineering (ICETCE) International Conference*, 1367-1370.
- Kim, S.M. and Abu Al-Rub, R.K. (2010). "Meso-scale computational modeling of the plastic-damage response of cementitious composites", *Cement and Concrete Research*, 41(3), 339-358.
- Mori, T. and Tanaka, K. (1973). "Average stress in matrix and average energy of materials with misfitting inclusions", *Acta Metallurgica*, 21, 571-574.
- Nguyen, T.T.H., Bary, B. and Larrard, T. (2015). "Coupled carbonation-rust formation-damage modeling and simulation of steel corrosion in 3D mesoscale reinforced concrete", *Cement and Concrete Research*, 74, 95-107.
- Özcan, D. M., Bayraktar, A., Sahin, A., Haktanir, T. and Tüker, T. (2009). "Experimental and Finite Element analysis on the steel fiber-reinforced concrete (SFRC) beams ultimate behavior", *Construction and Building Materials*, 23(2), 1064-1077.
- Qin, C. and Zhang, C. (2011). "Numerical study of dynamic behavior of concrete by meso-scale particle element modeling", *International Journal of Impact Engineering*, 38(12), 1011-1021.
- Rashid-Dadash, P. and Ramezani-pour, A.A. (2014). "Hybrid fiber reinforced concrete containing pumice and metakaolin", *Civil Engineering Infrastructures Journal (CEIJ)*, 47(2), 229-238.
- Rizzuti, L. (2014). "Effects of fibre volume fraction on the compressive and flexural experimental behaviour of SFRC", *Contemporary Engineering Sciences*, 7(8), 379-390.
- Roubin, E., Colliat, J. and Benkemoun, N. (2015). "Meso-scale modeling of concrete: A morphological description based on excursion sets of random fields", *Computational Materials Science*, 102, 183-195.
- Salehian, H., Barros, J.A.O. and Taheri, M. (2014). "Evaluation of the influence of post-cracking response of steel fiber reinforced concrete (SFRC) on load carrying capacity of SFRC panels", *Construction and Building Materials*, 73, 289-304.
- Shahabeyk, S., Hosseini, M. and Yaghoobi, M. (2011). "Meso-scale Finite Element prediction of concrete failure", *Computational Materials Science*, 50(7), 1973-1990.
- Skarzynski, L. and Tejchman, J. (2010). "Calculations of fracture process zones on meso-scale in notched concrete beams subjected to three-point bending", *European Journal of Mechanics*, 29(4), 746-760.
- Smilauer, V. and Bazant, Z. (2010). "Identification of viscoelastic C-S-H behavior in mature cement paste by FFT-based homogenization method", *Cement and Concrete Research*, 40(2), 197-207.

- Smilauer, V. and Krejci, T. (2009). "Multiscale model for temperature distribution in hydrating concrete", *International Journal for Multiscale Computational Engineering*, 7(2), 135-151.
- Sun, B., Wang, X. and Li, Z. (2015). "Meso-scale image-based modeling of reinforced concrete and adaptive multi-scale analyses on damage evolution in concrete structures", *Computational Materials Science*, 110, 39-53.
- Tailhan, J.L., Rossi, P. and Daviau-Desnoyers, D. (2015). "Probabilistic numerical modeling of cracking in steel fiber reinforced concretes", *Cement and Concrete Composites*, 55, 315-321.
- Teng, T.L., Chu, Y.A., Chang, F.A., Shen, B.C. and Cheng, D.S. (2007). "Development and validation of numerical model of steel fiber reinforced concrete for high-velocity impact", *Computational Materials Science*, 42(1), 90-99.
- Teng, T.L., Chu, Y.A., Chang, F.A. and Chin, H.S. (2004). "Calculating the elastic moduli of steel-fiber reinforced concrete using a dedicated empirical formula", *Computational Materials Science*, 31(3-4), 337-346.
- Titscher, T. and Unger, J.F. (2015). "Application of molecular dynamics simulations for the generation of dense concrete meso-scale", *Computers & Structures*, 158, 274-284.
- Ulm, F.J. and Jennings, H.M. (2008). "Does C-S-H particle shape matter? A discussion of the paper 'Modelling elasticity of a hydrating cement paste', by Julien Sanahuja, Luc Dormieux and Gilles Chanvillard, CCR 37 (2007) 1427-1439", *Cement and Concrete Research*, 38(8), 1126-1129.
- Wang, X., Yang, Z. and Jivkov, A.P. (2015). "Monte Carlo simulations of mesoscale fracture of concrete with random aggregate and pores: a size effect study", *Construction and Building Materials*, 80, 262-272.
- Wang, Z.L., Shi, Z.M. and Wang, J.G. (2011). "Analysis of post-cracking stage in SFRC elements through a non-linear numerical approach", *Engineering Fracture Mechanics*, 108, 238-250.
- Wang, Z.L., Konietzky, H. and Huang, R.Y. (2009). "Elastic-plastic-hydrodynamic analysis of crater blasting in steel fiber reinforced concrete", *Theoretical and Applied Fracture Mechanics*, 52(2), 111-116.
- Wang, Z.M., Kwan, A.K.H. and Chan, H.C. (1999). "Mesoscopic study of concrete I: Generation of random aggregate structure and Finite Element mesh", *Computers and Structures*, 70(5), 533-544.
- Williamson, G.R. (1974). "The effect of steel fibers on the compressive strength of concrete", *ACI Journal*, 44, 195-208.
- Wriggers, P. and Moftah, S.O. (2006). "Meso-scale models for concrete: homogenization and damage behavior", *Finite Elements in Analysis and Design*, 42(7), 623-636.
- Wu, M., Chen, Z. and Zhang C. (2015). "Determining the impact behavior of concrete beams through experimental testing and meso-scale simulation: I. Drop-weight tests", *Engineering Fracture Mechanics*, 135, 94-112.
- Xu, Z., Hao, H. and Li, H.N. (2012a). "Meso-scale modeling of dynamic tensile behavior of fiber reinforced concrete with spiral fiber", *Cement and Concrete Research*, 42(11), 1475-1493.
- Xu, Z., Hao, H. and Li, H.N. (2012b). "Meso-scale modeling of fiber reinforced concrete material under compressive impact loading", *Construction and Building Materials*, 26(1), 274-288.
- Yazici, S., Arel, H.S. and Tabak, V. (2013). "The effects of impact loading on the mechanical properties of the SFRCs", *Construction and Building Materials*, 41, 68-72.
- Zaitsev, Y.B. and Wittmann, F.H. (1981). "Simulation of crack propagation and failure of concrete", *Materials and Structures*, 14(2), 357-365.
- Zhang, J. (2013). "Three-dimensional modelling of steel fiber reinforced concrete material under intense dynamic loading", *Construction and Building Materials*, 44, 118-132.
- Zheng, J.J., Li, C.Q. and Zhou, X.Z. (2005). "Thickness of interfacial transition zone and cement content profiles between aggregates", *Magazine of Concrete Research*, 57(7), 397-406.
- Zhou, X.Q. and Hao, H. (2009). "Mesoscale modeling and analysis of damage and fragmentation of concrete slab under contact detonation", *International Journal of Impact Engineering*, 36(12), 1315-1326.
- Zhou, X.Q. and Hao, H. (2008a). "Meso-scale modeling of concrete tensile failure mechanism at high strain rates", *Computers & Structures*, 86(21-22), 2013-2026.
- Zhou, X.Q. and Hao, H. (2008b). "Modeling of compressive behavior of concrete-like materials at high strain rate", *International Journal of Solids and Structures*, 45(17), 4648-4661.